



EUROPEAN ORGANIZATION FOR NUCLEAR RESEARCH

CERN-EP/88-22  
February 29th, 1988

ASYMMETRY IN  $\bar{p}p$  ELASTIC SCATTERING

R.A.Kunne <sup>1,\*</sup>), C.I.Beard <sup>2,\*\*</sup>), R.Birsa <sup>3</sup>), K.Bos <sup>1</sup>),  
F.Bradamante <sup>3</sup>), D.V.Bugg <sup>2</sup>), A.S.Clough <sup>4</sup>),  
S.Dalla Torre-Colautti <sup>3</sup>), S.Degli-Agosti <sup>5</sup>), J.A.Edgington <sup>2</sup>),  
J.R.Hall <sup>2,†</sup>), E.Heer <sup>5</sup>), R.Hess <sup>5</sup>), J.C.Kluyver <sup>1</sup>),  
C.Lechanoine-Leluc <sup>5</sup>), L.Linssen <sup>1,\*\*</sup>), A.Martin <sup>3</sup>),  
T.O.Niinikoski <sup>6</sup>), Y.Onel <sup>5,\*\*\*</sup>), A.Penzo <sup>3</sup>), D.Rapin <sup>5</sup>),  
J.M.Rieubland <sup>6</sup>), A.Rijllart <sup>6</sup>), P.Schiavon <sup>3</sup>), R.L.Shypit <sup>4,††</sup>),  
F.Tessarotto <sup>3</sup>), A.Villari <sup>3</sup>) and P.Wells <sup>2</sup>)

Abstract

Asymmetries  $A_{0n}$  have been measured at LEAR for  $\bar{p}p$  elastic scattering for 15 beam momenta from 497 to 1550 MeV/c using a polarized target.  $A_{0n}$  is defined as  $(\sigma^+ - \sigma^-) / (\sigma^+ + \sigma^-)$ , where  $\sigma^+$  resp.  $\sigma^-$  are the differential cross sections for target polarization up resp. down.

(Submitted to Physics Letters B)

- 
- 1) NIKHEF-H, Amsterdam, The Netherlands
  - 2) Queen Mary College, London, England
  - 3) INFN Trieste and University of Trieste, Trieste, Italy
  - 4) University of Surrey, Guildford, Surrey, England
  - 5) DPNC, University of Geneva, Geneva, Switzerland
  - 6) CERN, Geneva, Switzerland

\*) Present address: DPNC, University of Geneva, Geneva, Switzerland

\*\*\*) Present address: CERN, Geneva, Switzerland

\*\*\*) Present address: University of Iowa, Iowa City IA, USA

†) Present address: BNL, Upton NY, USA

††) Present address: JPL, Pasadena CA, USA

The availability of clean, intense antiproton beams at LEAR allows a considerable improvement in data on  $\bar{p}p$  elastic scattering. We report the measurement of  $A_{0n}$  over as much ~~of~~ the angular range as can be achieved with a conventional polarized target.

Although precise measurements of the differential cross sections are already available for momenta below 2000 MeV/c [1] [2] [3], there exists only one measurement of the asymmetry in this momentum range. The latter, reported by Albrow et al. [4] in the momentum range from 910 to 2500 MeV/c, suffers from poor statistics beyond the first diffraction minimum. The results presented here allow a first clear view of the physics beyond this point and should therefore be useful in improving potential models.

From our data the differential cross sections can also be derived, but this analysis is still in progress. Preliminary results have been submitted to the IV LEAR Workshop in Villars [5], and agree with the data of Ref. [1].

The experimental setup is sketched in figure 1. The target was a 3 cm long cylinder, 1 cm in diameter, containing pentanol ( $C_5H_{11}OH$ ), equivalent to 3.7 cm of liquid hydrogen. Its polarization, typically 75%, was monitored by standard NMR techniques with a reproducibility of  $\pm 0.5\%$ , and an estimated absolute accuracy of  $\pm 4\%$ . A dummy target containing teflon ( $(CF_2)_n$ ) and a  $LH_2$  target for background studies and absolute normalization of cross sections respectively, were also used. The targets were placed in the nose of a cryostat situated in the gap of a C-shaped dipole magnet.

Immediately around the target but still in the gap of the magnet were a J and a C shaped MWPC. Further out were two MWPCs -each shaped as part of a cylinder- one on the left side and one on the right side of the through-going beam. The chambers all had two planes of vertical wires to provide information about the horizontal coordinate and two planes of cathode read-out strips to provide the vertical coordinate.

Two veto counters that rejected annihilation events, were mounted horizontally in the gap of the magnet, just above and below the target.

The trajectory of the incoming beam particle was defined by two MWPCs, each having a vertical and a horizontal wireplane. The beam trigger was given by a coincidence of three beam counters. The first one, S0, was placed 24 meters upstream of the target at an intermediate focus. The second, S1, was located just inside the right outer chamber. The smallest one, S2, was situated just upstream of the target; it was 1 mm thick and had a diameter of 10 mm. It was aligned on the target by transmission measurements.

The beam intensity was typically  $10^5/s$ . The momentum spread in the target around the central value increased from 1.8 MeV/c at the highest momentum to 10.2 MeV/c at the lowest momentum. At the lowest momenta the beam filled the aperture of the defining scintillator.

The MWPCs were surrounded by two arrays of eight respectively nine scintillation counters. These counters were part of the event trigger. They selected two-body candidate events with approximately the correct kinematics. A second level trigger, using the hits in the two outer MWPCs, refined this selection. Because of the 2.5 T magnetic field the geometry was quite different for events where the antiproton scattered to the left ( $\bar{p}p$ ) or to the right ( $p\bar{p}$ ), as illustrated in figure 1. Both the outer chambers and the trigger scintillators could be rotated around the magnet, permitting the optimal angular range of two-body reactions to be covered at each momentum.

Events were identified off-line using a reconstruction procedure which fitted complete two-body events to the chamber hits. This method is described in [6]. It obtained the parameters of the reaction (vertex position  $v_x$ ,  $v_y$  and  $v_z$ ; polar and azimuthal scattering angles  $\theta_{cm}$ ,  $\phi_{cm}$ ; beam

inclinations  $\alpha_h$  and  $\alpha_v$ ) and assigned to each event candidate a goodness of fit parameter  $\chi^2$  per degree of freedom ( $\chi^2/DF$ ). A cut on the longitudinal vertex position ( $|v_z| < 12$  mm) assured that the events were well inside the target. Typical resolutions of the reconstructed parameters (at 1089 MeV/c) are:  $\pm 0.3$  mm for  $v_x$  and  $v_z$ ,  $\pm 2$  mm for  $v_y$ ,  $\pm 0.5^\circ$  for  $\theta_{cm}$  and  $\pm 1^\circ$  for  $\phi_{cm}$ . The background of events from carbon and oxygen was evaluated from runs with the dummy target at three momenta (523, 1089 and 1434 MeV/c). The shape of this background varied little with momentum and  $\theta_{cm}$ . It was normalized to the pentanol data for  $\chi^2/DF > 10$ . At intermediate momenta the background was estimated by interpolation. However, an alternative method that uses the shape of the dummy target data closest in momentum, gave almost identical results. The background subtracted under the signal peak ( $\chi^2/DF < 10$ ) amounted to 10-15% of the remaining events (figure 2). A check on the whole procedure of reconstruction and background subtraction was that asymmetries in the forward direction agree within errors for the two scattering geometries ( $\bar{p}p$  and  $p\bar{p}$ ), although the geometry and the background for these two channels are quite different. One example of the difference in the asymmetry obtained from the two samples is shown in figure 3. The  $\chi^2/DF$  with respect to zero of these differences is about 1.5 for all momenta. From momentum to momentum no systematic trend is seen.

Results (combined for  $\bar{p}p$  and  $p\bar{p}$ ) are shown in figure 4. (Numerical values are available on request from the first author.) The quoted momenta are those at the centre of the target. The acceptance increases from  $-0.28 < \cos \theta < 0.28$  at 497 MeV/c to  $-0.84 < \cos \theta < 0.80$  at 1550 MeV/c. Arrows give the positions of the diffraction minima in our differential cross section data. The data show the rich structure already noticed by Daum et al. [7] and interpreted in terms of the Frahn and Venter optical model [8], which could well reproduce the diffractionlike pattern exhibited by the differen-

tial cross section. Our data have a factor of five better statistics than [4] and are not compatible with this simple optical model description. In fig. 4 they are compared with model predictions from the Paris model [9] and the Dover-Richard model (second parametrization) [10].

We acknowledge gratefully the assistance of CERN, in particular the LEAR operating crew.

## References

- [1] E.Eisenhandler et al., Nucl. Phys. B113 (1976) 1 for 690  $\langle p_{lab} \rangle$  2430 MeV/c.
- [2] W.Bruckner et al., Phys. Lett. 166B (1986) 113 for 180  $\langle p_{lab} \rangle$  600 MeV/c.
- [3] T.Kageyama et al., Phys. Rev. D35 (1987) 2655 for 390  $\langle p_{lab} \rangle$  780 MeV/c.
- [4] M.G. Albrow et al., Nucl. Phys. B37 (1972) 349.
- [5] C.I.Beard et al., in: Proceedings of the IV LEAR Workshop, Villars-sur-Ollon 1987 (to be published).
- [6] E.Aprile et al., in: CERN 81-07, p.124-131.
- [7] C.Daum et al., Nucl. Phys. B6 (1968) 617.
- [8] W.H.Frahn and R.H.Venter, Ann. of Phys. 27 (1964) 135, 385, 401.
- [9] J.Cote et al., Phys. Rev. Lett. 48 (1982) 1319.
- [10] C.Dover and J.M.Richard, Phys. Rev. C21 (1980) 1466.

Figure captions.

Figure 1: Schematic view of the experimental setup. S0,S1,S2: beam defining counters; B,J,C,L,R: multiple wire proportional chambers; HL,HR: hodoscope counters; M: polarized target magnet; P: cryostat with polarized target; beam: incident and throughgoing beam track;  $\bar{p}p$ : approximate accepted angular range,  $\theta_{cm}$ , antiprotons to the left;  $p\bar{p}$ : same for protons to the right.

Figure 2: Signal and background (dashed histogram) as a function of  $\chi^2$  per degree of freedom for 1089 MeV/c. Background normalized to signal for  $\chi^2/DF > 10$ .

Figure 3: Difference  $A_{on}(p\bar{p}) - A_{on}(\bar{p}p)$  obtained from the two geometries ( $\bar{p}p$  and  $p\bar{p}$ ) at 1089 MeV/c.

Figure 4: Asymmetries for momenta from 497 to 1550 MeV/c. Full curve: prediction from the Paris potential model [9]. Dashed curve: prediction from the second Dover-Richard model [10], which is not applicable for momenta above 1 GeV/c. Arrows give the position of the diffraction minima as seen in our differential cross section data.

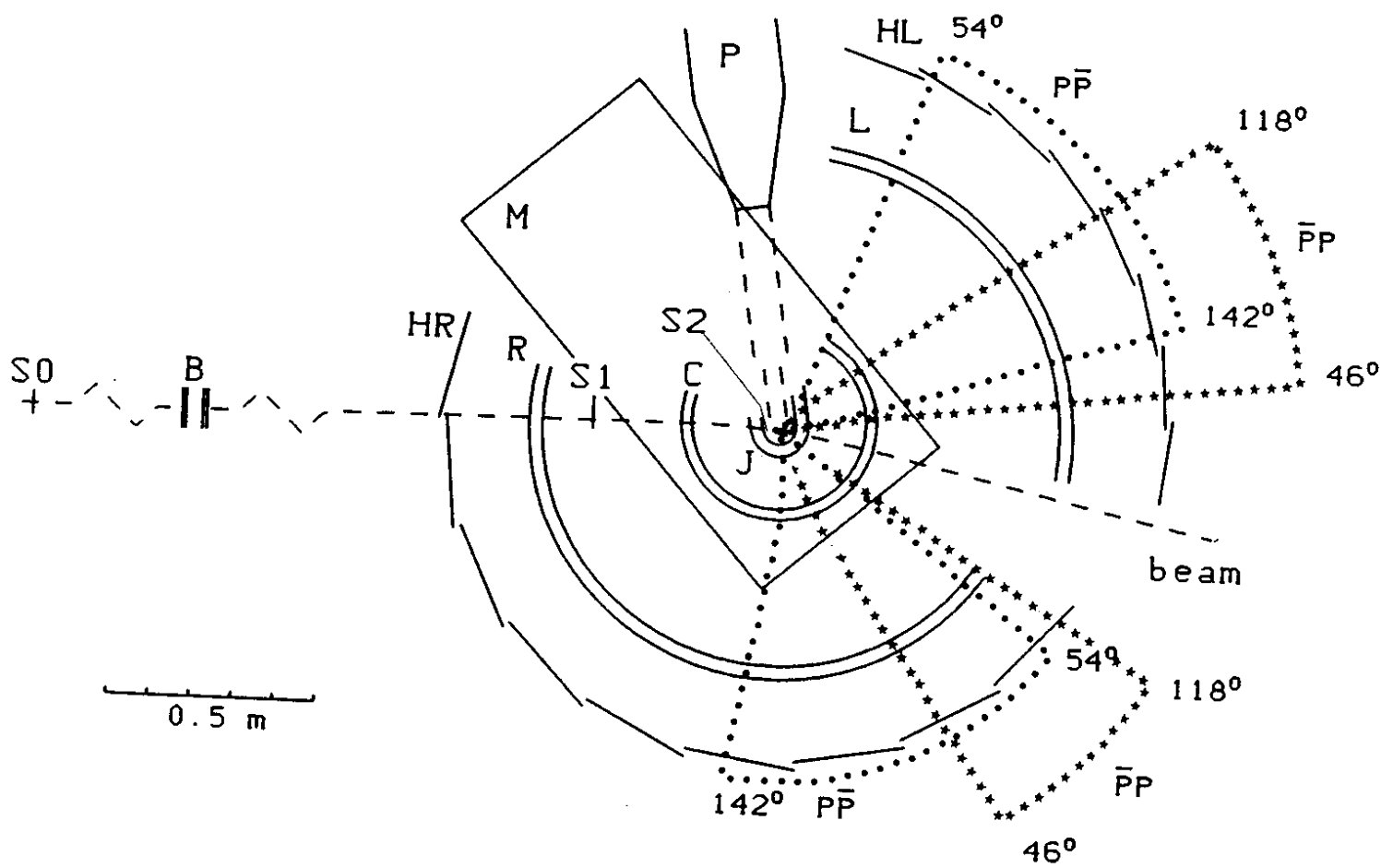


Figure 1



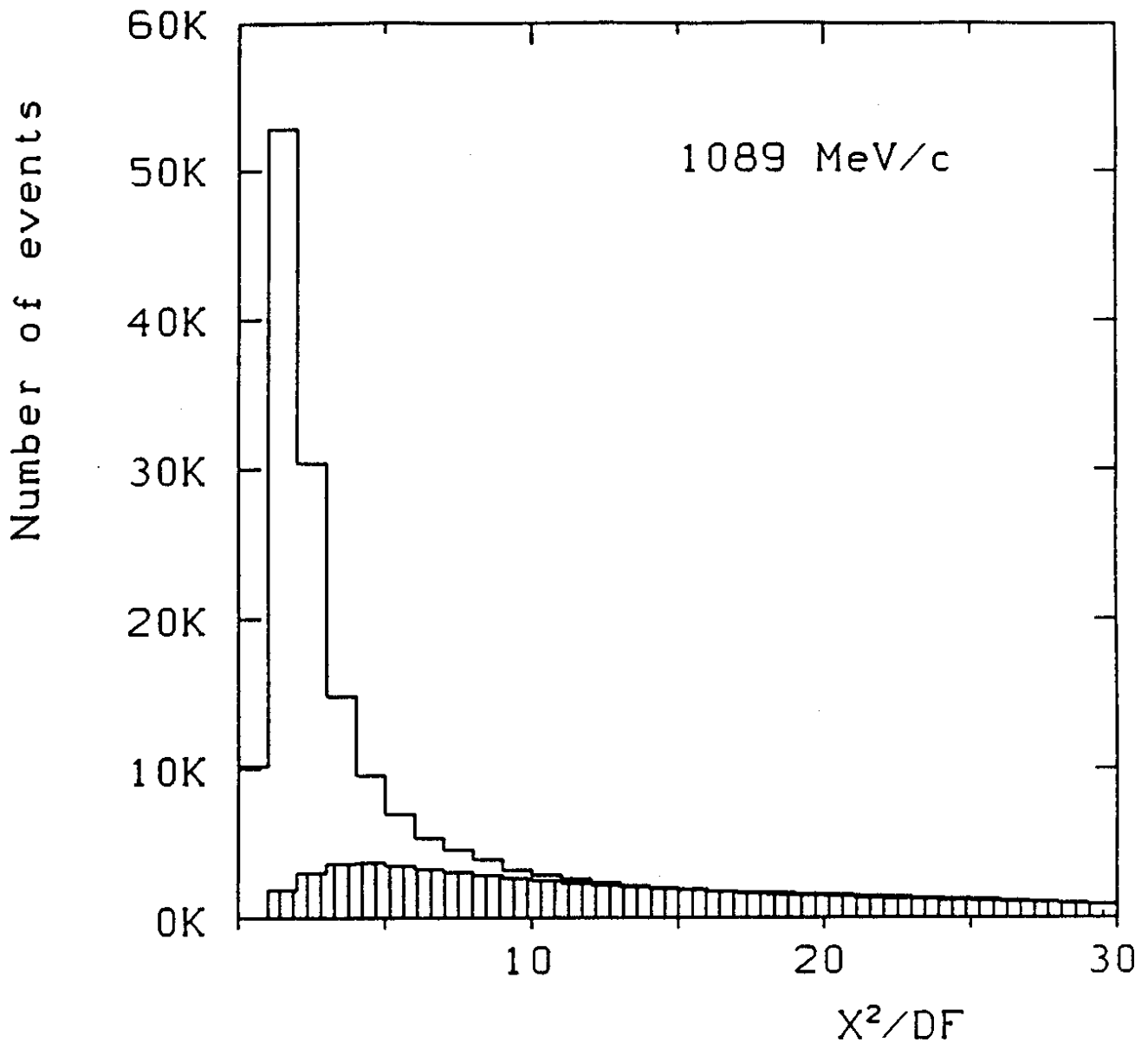


Figure 2

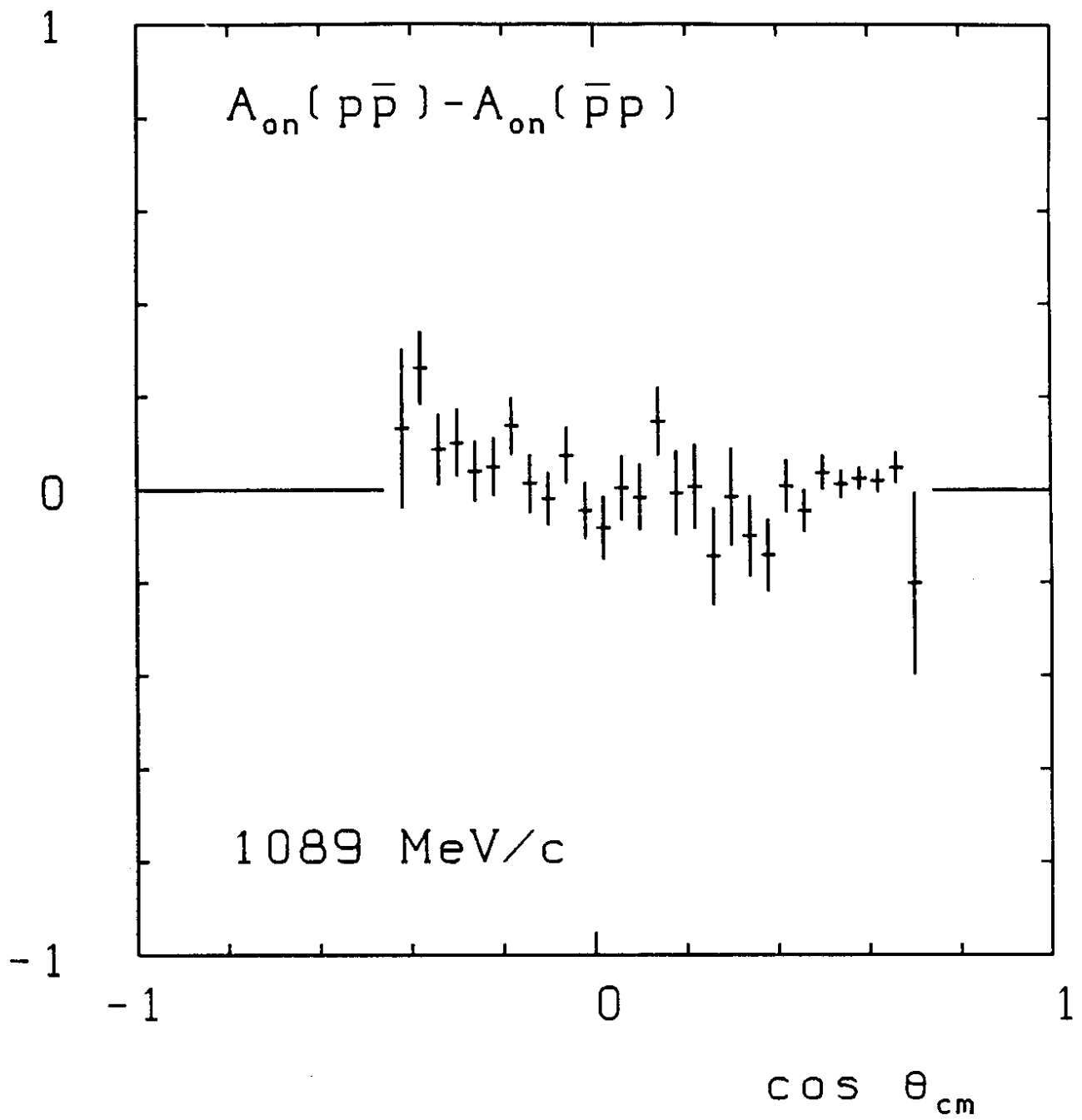


Figure 3

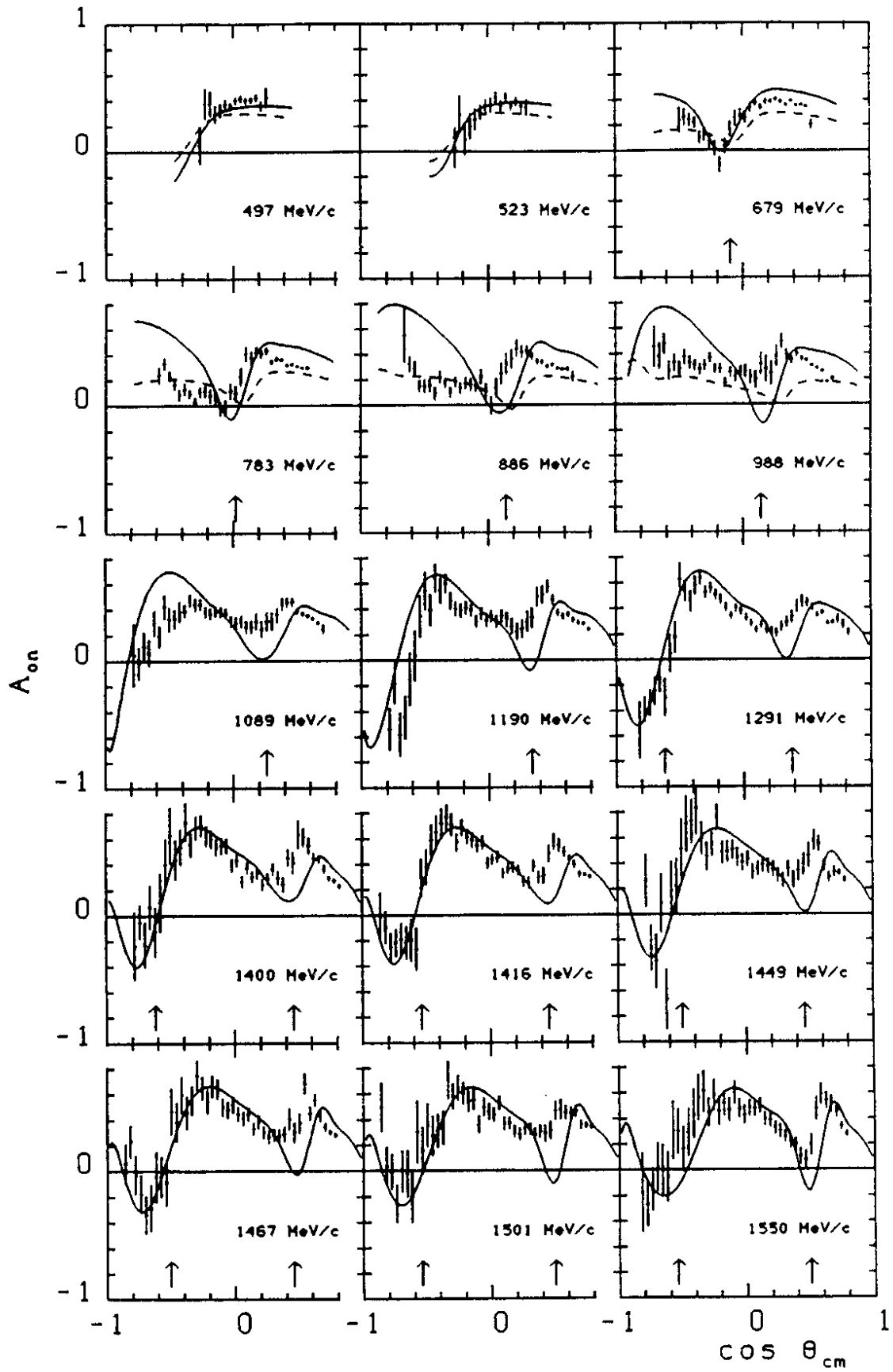


Figure 4.